Progress In Electromagnetics Research B, Vol. 56, 1–24, 2013

FINITE ELEMENT MODELING OF SELECTIVE HEATING IN MICROWAVE PYROLYSIS OF LIGNOCELLULOSIC BIOMASS

Baishali Dutta[1, *], Satyanarayan R. S. Dev[2], and Vijaya G. S. Raghavan[1]

[1]Department of Bioresource Engineering, McGill University, 21111 Lakeshore Road, Ste-Anne-de-Bellevue, QC, H9X 3V9, Canada

[2]College of Applied Sciences, A'Sharqiyah University, P. O. Box 42, Postal Code 400, Ibra, Sultanate of Oman

Abstract—Microwave pyrolysis overcomes the disadvantages of conventional pyrolysis methods by efficiently improving the quality of final pyrolysis products. Biochar, one of the end products of this process is considered an efficient vector for sequestering carbon to offset atmospheric carbon dioxide. The dielectric properties of the doping agents (i.e., char and graphite) were assessed over the range of 25°–400°C and used to develop a finite element model (FEM). This model served to couple electromagnetic heating, combustion, and heat and mass transfer phenomena and evaluated the advantages of selective heating of woody biomass during microwave pyrolysis. The dielectric properties of the doping agents were a function of temperature and decreased up to 100°C and thereafter remained constant. Regression analysis indicated that char would be a better doping substance than graphite. The simulation study found that doping helped to provide a more efficient heat transfer within the biomass compared to non-doped samples. Char doping yielded better heat transfer compared to graphite doping, as it resulted in optimal temperatures for maximization of biochar production. The model was then validated through experimental trials in a custom-built microwave pyrolysis unit which confirmed that char doping would be better suited for maximization of biochar.

Received 25 August 2013, Accepted 16 October 2013, Scheduled 22 October 2013

* Corresponding author: Baishali Dutta (baishali.dutta85@gmail.com).

1. INTRODUCTION

Combating global climate change and meeting the world's ever-rising energy demands are twin concerns which challenge researchers all around the world. Evidence strongly supports the occurrence of climate change, based on a wide range of indicators including increases in global average air and ocean temperatures, widespread melting of snow and ice, and rising global sea levels. Carbon dioxide tends to accumulate in the atmosphere for a long time and with continued anthropogenic emissions, CO_2 levels will only continue to build-up in the atmosphere. The Intergovernmental Panel on Climate Change (IPCC) Fourth Assessment Report suggests that even with significant reductions in anthropogenic CO_2 emissions, atmospheric CO_2 levels would only very gradually decline as natural processes slowly removed CO_2 from the atmosphere [1]. Therefore past anthropogenic CO_2 emissions will continue to have a destabilizing impact on earth's climate system for a very long time. Climate change has irreversible effects on our economy, infrastructure, and health, the landscapes around us, and the wildlife that inhabit them.

Although climate change has been attributed to both natural processes and human activities, a recent heightening of public awareness regarding greenhouse gases' role in global warming has led to a greater scrutiny of such contributory activities as CO_2 emissions from carbon-based fossil fuel combustion, rising population and irresponsible acts of deforestation and land use. In Canada, over 80% of total national greenhouse gas emissions are associated with the production or consumption of fossil fuels for energy purposes [2].

Canada's total GHG emissions for 2011 were estimated at 702 Mt of CO_2 equivalents (CO_2e), of which nearly 8% was contributed by the agricultural sector [3]. This sector generates roughly 300 Mt of agricultural waste [4, 5]. Assuming 50% recovery of carbon from this biomass, one could sequester nearly 150 Mt of carbon dioxide from the atmosphere, in the form of biochar, or about 20% of Canada's GHG emissions.

An increased need for technologies with long-term sustainability implications for the bioenergy sector has been widely acknowledged. Biochar's use as an energy source [6], as a fertilizer when mixed with soil [7], and as a means of reducing greenhouse gas emissions through the soil-sequestration of carbon [8], have led to its gaining significant attention in recent years. Moreover, biochar can increase food security by reducing the amount of food crops used for biofuel production [9].

One of the most important thermochemical biomass-conversion technologies, pyrolysis is a process of thermal decomposition of biomass

under conditions ranging from low oxygen ($< 1\%$ O_2 v/v) to anoxia. It converts organics to solid (charcoal), liquid (organics) and gaseous (CO, CO_2, CH_4, H_2) products. Their range and relative amounts depend on process variables such as the nature of the feedstock and the heating rate [10, 11]. Biochar production through pyrolysis has become an extremely efficient and popular technology in recent years [12].

Conventional pyrolysis techniques have a few inherent disadvantages such as poor heating characteristics in the core of the biomass as well as being time consuming. One of the methods proven to have measured up to good efficiency and potentially negate the disadvantages of conventional methods is the use of microwave or microwave-assisted pyrolysis methods to generate biochar. The application of microwaves to produce biochar has been proven to enhanced biochar yield and quality, and, to a large extent, negate undesirable secondary reactions among volatile compounds. In addition it is a rapid and energy-efficient technology compared to conventional methods [11]. One of the driving principles of microwave heating is based on 'molecular friction' (or dielectric loss) [13]. The principles of dielectric heating as opposed to that of conventional heating can be best summarized through Figure 6 below. Dielectric heating of a material causes thermal effects which may cause a different temperature regime within the material [14]. The biomass is heated by conduction from the surface to its core in the conventional method and by convective heat transfer from high-temperature gas. The temperature at the surface of the biomass is known to be higher than that at the core because of the poor thermal conductivity of lignocellulosic biomass. Hence as the dielectric properties govern the ability of materials to heat in microwave fields, the measurement of these properties as a function of other relevant parameters such as frequency, temperature, moisture content, etc. is important [15].

There is a growing interest in modeling and simulation studies regarding the production of biochar as well other pyrolysis by-products. Numerical and modeling studies have been conducted which focus on estimation of optimum parameters in pyrolysis of biomass [16]. Different approaches used in the transport models have also been presented at both the single particle and reactor levels, together with the main achievements of numerical simulations [17].

There is poor understanding of the mechanisms involved in application of electromagnetic energy for the pyrolysis of biomass and the actual energy distribution inside the biomass when subjected to electromagnetic fields [18]. The electromagnetic field distribution inside a microwave oven can be traced out by solving Maxwell's equations. Finite Element Method (FEM) is commonly used for

solving Maxwell's equations to obtain the energy distribution in a complex object or within a multimode cavity. It is capable of simulating power density distribution in 3-D space [19].

FEM technique competes very favorably with the other numerical methods, as it is based on reducing the Maxwell's equations to a system of simultaneous algebraic linear equations [20]. FEM can readily model heterogeneous and anisotropic materials as well as arbitrarily-shaped geometries. It can also provide both time and frequency domain analyses which are important to microwave heating problems like field distribution, scattering parameters and dissipated power distribution for various materials and geometries [21].

The addition of microwave receptors has been found to improve heat distribution in biological materials during microwave processing. Sanga et al. (2000) investigated microwave and hot air drying characteristics of special cases of biological material (carrots) and compared their drying rates, surface color, re-hydration capacity and shrinkage. The samples were inserted with teflon at core center of carrots were dried by microwave and hot air drying. It was found that microwave drying of the special case biological material (carrot embedded with teflon) had higher drying rates and less shrinkage. Re-hydration capacity of biological material dried as a special case was also found to higher than those dried as standalone under the same drying conditions [22].

Many researchers have concluded that the optimum pyrolysis conditions for by product maximization cannot be attained without adding a microwave-susceptible doping agent which has been found to have significant impact on the pyrolysis conditions and the products formed [23, 24]. The goals of using a doping agent are to absorb maximum microwave radiation in the initial phase and then to help sustain the pyrolysis process and final temperatures [25]. The dielectric properties of a microwave-susceptible doping agent are an important factor in its selection for microwave assisted pyrolysis as it determines the extent to which the doping agent will influence the heating mechanism.

1.1. Previous Simulation Results

Dutta et al. [18] showed lignocellulosic biomass (wood) that the highest yield of biochar was found to be at 425°C at a power density of 7.5 W/g and was found to be optimum for pyrolysis of lignocellulosic biomass for maximization of biochar. An evidence of non uniform heating resulting in the creation of hot spots in the biomass was observed through the experimental validation of the simulation of the microwave pyrolysis. Although the biochar yield was found to in agreement with

the simulation results, the pyrolysis process was hard to control due to the non uniformity of heating and the generation of sparks in the cavity [18].

Taking these facts into account, the dielectric properties of char and graphite were determined in order to select the doping agent best suited to maximize biochar yield of biochar through microwave pyrolysis. A Finite Element Model (FEM) of the microwave pyrolysis of lignocellulosic biomass was developed. Simulation studies were conducted for biomass doped with char and graphite and subjected to microwave pyrolysis at a frequency of 2.45 GHz and slow heating conditions as illustrated in Dutta et al. (2010) in order to visualize and investigate energy distribution within the biomass [18]. The simulation results of the microwave heating mechanism and profile obtained for the doped biomass was compared to that of the dope-free sample.

2. MATERIALS AND METHODS

2.1. Nomenclature

Symbol	Property
k	Kinetic reaction constant (s^{-1})
A_x	Arrhenius constant (s^{-1})
E_a	Activation energy of reaction (kJ mol^{-1})
Pav	Time average power dissipated (W)
ρ	Density of the material (kg m^{-3})
Cp	Specific heat capacity of the material (kJ kg^{-1} $^{\circ}K^{-1}$)
K	Thermal conductivity (W m^{-2} $^{\circ}K^{-1}$)
Q	Power Source Term (W m^{-3})
V	Volume (m^3)
E	Total Electric field intensity (V m^{-1})
E_x	Electric field intensity x component (V m^{-1})
E_y	Electric field intensity y component (V m^{-1})
E_z	Electric field intensity z component (V m^{-1})
H	Total Magnetic Field Intensity (A m^{-1})
H_x	Magnetic field intensity x component (A m^{-1})
H_y	Magnetic field intensity y component (A m^{-1})
H_z	Magnetic field intensity x component (A m^{-1})

2.2. Dielectric Properties Measurement

The dielectric properties for char of lignocellulosic origins (willow wood) and graphite obtained from a local store (DeSerres, Montreal, Canada) were evaluated. The dielectric constant (ε') and dielectric loss factor (ε'') were measured using an Agilent 8722 ES s-parameter Network Analyzer equipped with a high temperature probe (model 85070B) and controlled with the Agilent 85070D Dielectric Probe Kit Software (Version E01.02) operating at 2.45 GHz.

Using a furnace, samples of char and graphite were heated to temperatures in the range of 50–400°C prior to measurements being taken. Measurement of the frequency shift and change in quality factor was made at selected resonant frequencies. The dielectric properties of the sample were measured at each temperature through the network analyzer.

According to the manufacturer, the equipment has an accuracy of ±5% for the dielectric constant (ε') and ±0.005% for the loss factor (ε'') (HP 1992). A diagram of the experimental setup used for the measurement of dielectric properties is shown in Figure 1.

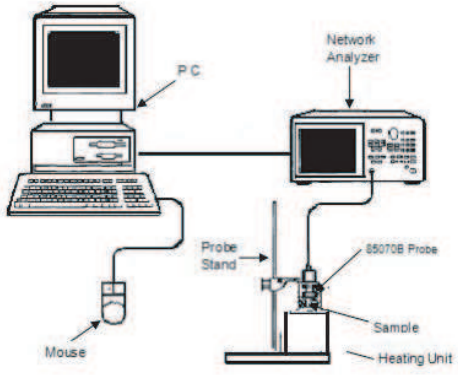

Figure 1. Dielectric properties measurement unit.

2.3. Microwave Pyrolysis Set-up for Experimental Validation

The experimental validation of the simulation results was carried out in a custom-built microwave pyrolysis unit within a regular domestic multimode microwave oven operating at 2.45 GHz, with cavity dimensions of 205 mm × 335 mm × 180 mm located in the

laboratories of the Department of Bioresource Engineering, McGill University.

The quartz pyrolysis bioreactor system used for the simulation (Figure 2) consisted of three parts: an upper cylinder (40 mm inner diameter, 90 mm height), a lower cylinder (50 mm inner diameter, 42 mm height) and a sample stand (35 mm diameter, 25 mm height). Through two quartz tubes, one inlet, one outlet (each 6.3 mm diameter, 25.4 mm length) air inside the reactor was purged with nitrogen at a flow rate of 0.003 L s^{-1} to create an oxygen-free inert atmosphere.

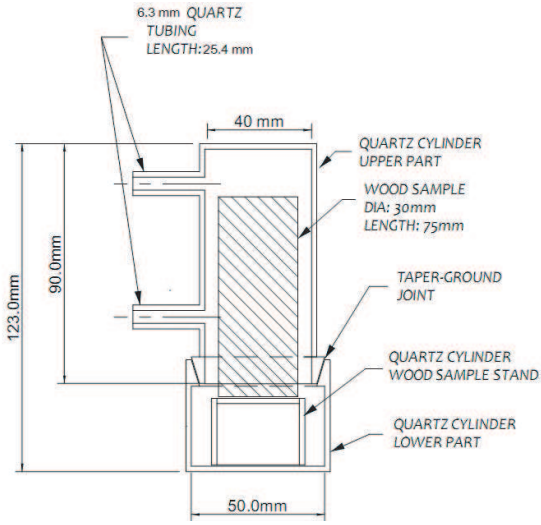

Figure 2. Microwave pyrolysis bioreactor setup.

The reactor was placed in the middle of the microwave chamber and the two quartz tubes connected to the nitrogen gas supply and gaseous product release. A K-type thermocouple was inserted into the reactor through the gaseous product release tube to monitor the biomass temperature continuously throughout the experiment. The gaseous product release pipe was connected to a condensation unit continuously rotated in cooling water at $\leqslant 10°C$. In order to validate the simulation model, an experimental design with temperature as the single factor and triplicate samples was chosen. Three temperatures for each of the experimental set up were selected as Table 1.

Each pyrolysis run ended 15 min after the start of irradiation. After each run, the reactor was cooled to ambient temperature under a nitrogen atmosphere. The biochar remaining in the reactor was weighed to compare yields.

Table 1. Experimental conditions for experimental validation.

Experimental set up	Temperature
Doping type (Non doped, Graphite, Char)	250
	290
	330

2.4. Sample Preparation

The biomass taken into consideration for simulation was maple wood (30 mm diameter, 75 mm length) with a moisture content of $\simeq$ 7%. This was mounted on the sample stand. It was theoretically assumed that the biomass sample was doped with char or graphite of 30 mm diameter and 75 mm length having the dielectric properties determined in separate simulations in a prior experiment. The wood sample was then subjected to microwave heating at a 2.45 GHz frequency and power density of 7.5 W g^{-1} for simulation purposes. The thermal properties of the maple wood, char and graphite used for the simulation have been provided in Table 2.

Table 2. Thermal properties of sample materials used for simulation purpose.

Properties	Wood	Char	Graphite
Thermal conductivity (W/mK)	0.8 [26]	150 [27]	
Density (kg/m^3)	640 [26]	280 [27]	1950 [27]
Specific heat capacity (constant pressure) (KJ/kg K)	1.63 [26]	1 [28]	0.71 [28]
Relative permittivity (ε_r)	1 [29]	1 [29]	10 – j
Relative permeability (μ_r)	1 [30]		

2.5. Development of the Mathematics and Governing Equations for Microwave Assisted Pyrolysis

2.5.1. Formulation of the Equations for the Electromagnetic Field [11]

2.5.1.1. Electromagnetics

The Maxwell's equations that govern the electromagnetic phenomena evolving in a given configuration resolved in 3D space were solved for the electric field intensity, E (V m^{-1}), and magnetic

field intensity, H (A m^{-1}). At the macroscopic level, electromagnetic phenomena were defined using Maxwell Equations.

For the simulation of the biomass pyrolysis in the microwave environment, the Maxwell equations, which govern the electric (E) and magnetic (H) fields decouple polarization state of transverse electric mode (TE) [31]. The electromagnetic field distribution inside the microwave oven was traced out by solving the following Maxwell's equations [32]:

The time averaged power dissipation (P_{av}) in each element in a dielectric material was obtained by integrating the Poynting vector (P_c) over the closed surface S for each tetrahedral element (Equation (1)) [18].

$$P_{av} = -\frac{1}{2}\int_S P_c \cdot dS \tag{1}$$

where $P_c = E \times H$.

Volumetric heat generation (Q) can be expressed in terms of power intensity in three orthogonal directions [15]:

$$Q = \frac{\partial P_{av(x)}}{\partial V} + \frac{\partial P_{av(y)}}{\partial V} + \frac{\partial P_{av(z)}}{\partial V} \tag{2}$$

where the suffixes x, y and z indicate time average power dissipated in the corresponding directions and where V is the volume in which the heat is generated.

The dynamically changing dielectric constant ε' and loss factor ε'' were calculated using equations derived from the measurement of dielectric properties (Equation (3)).

$$\varepsilon = \varepsilon' - j\varepsilon'' \tag{3}$$

And the loss tangent is:

$$\tan\delta = \frac{-\varepsilon''}{\varepsilon'} \tag{4}$$

2.5.1.2. Boundary Conditions

Perfect Electrical Conductor (PEC) boundary condition ($n \times E = 0$) was used for the walls of the cavity and Perfect Magnetic Conductor (PMC) boundary condition ($n \times H = 0$) was used for the symmetry boundaries.

Boundary conditions at the port were taken as follows:

$$H_y = A\cos\left(\frac{\Pi x}{\alpha}\right)\cos(\omega t + \beta t) \tag{5}$$

$$E_z = \frac{\omega\mu_0\alpha}{\Pi}A\sin\left(\frac{\Pi x}{\alpha}\right)\sin(\omega t + \beta t) \tag{6}$$

$$H_x = \frac{\beta\alpha}{\Pi} A \sin\left(\frac{\Pi x}{\alpha}\right) \sin(\omega t + \beta t) \tag{7}$$

where the x, y and z coordinates indicate the corresponding axes, and A is the cross sectional area of the waveguide, ω is the phase angle and α and β are arbitrary constants.

Thermal boundary conditions: The surface of the cylindrical wood sample was used as the thermal boundary conditions for the simulation. Surface to ambient boundary conditions were applied for the circumference of the sample in order to simulate the heating mechanism inside the quartz reactor.

Heat transfer [11]

The thermal energy equation is given as [32]:

$$\rho C_p \frac{\partial T}{\partial t} = \nabla \cdot (K \nabla T) + Q \tag{8}$$

$$\nabla \times \mu_r^{-1} (\nabla \times E) = k_0^2 \left(\varepsilon_r - \frac{j\sigma}{\omega \varepsilon_0}\right) E \tag{9}$$

where, ρ is the density (kg m^{-3}), C_p is the specific heat (kJ kg^{-1} °K^{-1}), K is the thermal conductivity of the material (W m^{-2} °K^{-1}), and T is the absolute temperature (°K).

Different mesh element sizes were used for different sub-domains based on the dielectric properties of the sub-domain and the precision required in the sub-domain of interest.

Taking all the above into consideration, a Finite Element Model (FEM) of the microwave pyrolysis of lignocellulosic biomass is an

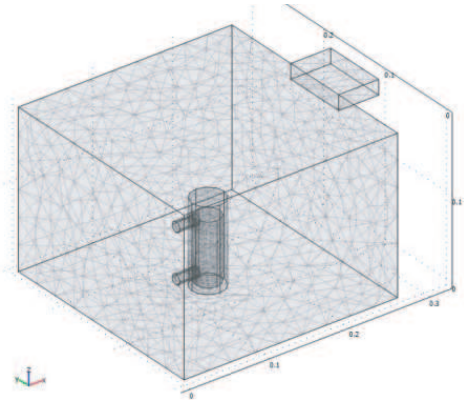

Figure 3. Finite element mesh structure of the microwave pyrolysis unit for simulation.

optimum numerical approximation technique for MWP [17]. The resulting sets of partial differential equations were then simultaneously solved using the COMSOL Multiphisics software package (ver. 4.1a, COMSOL Inc., USA) [33].

With this software a 3D Finite Element Model was developed to simulate the microwave pyrolysis process for a regular domestic multimode microwave oven configuration. The meshed structure of the microwave cavity along with the bioreactor and wood sample are shown in Figure 3. A custom-built computer with two AMD Opteron quadcore 2.4 GHz processors and 32 GB primary memory was used to run the simulations.

3. RESULTS AND DISCUSSION

3.1. Dielectric Properties

The dielectric properties of char and graphite were found to be consistently uniform at temperatures above 200°C (Figure 4). The dielectric constant (ε') of biochar and graphite decreased linearly up to 100°C and remained constant thereafter. The dielectric loss factors of both graphite and char were negligible and remained constant across the entire range of temperature.

A linear regression model was applied to the dielectric properties of both char and graphite to analyze their relationship to temperature. The dielectric loss (ε'') values of both the biochar and graphite did not change significantly with respect to temperature ($P > 0.05$). Changes in ε'' values remained relatively negligible with increases in temperature and hence did not fit a linear model.

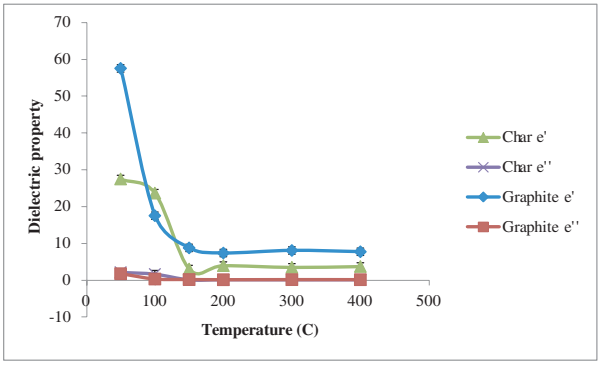

Figure 4. Change in dielectric properties of char and graphite with varying temperatures at 2450 MHz.

The ε' for both char and graphite decreased with increasing temperature. A linear additive model was used to relate ε' to temperature with a general form of:

$$\varepsilon' = a \pm bT \tag{10}$$

where, T is the temperature in °C, and a and b are model coefficients.

The regression analysis performed on the collected data yielded the following relationships for char and graphite respectively:

$$\varepsilon'_{\text{char}} = 37.35 - 0.182T \tag{11}$$

$$\varepsilon'_{\text{graphite}} = 62.62 - 0.32T \tag{12}$$

The coefficient of determination (R^2) value of the dielectric constant values for char and graphite were 0.77 and 0.73 respectively ($P \leqslant 0.05$; Figures 5 and 6). These models are useful in determining the dielectric properties of char or graphite at any given temperature within the range studied.

The results of the present investigation of the dielectric properties of char produced from wood and graphite concur with the findings of Robinson et al. who compared the dielectric loss for < 1 mm wood pellets, dried at 105°C and with 6.3% water content over a temperature range of 25° to 800°C. Their study also showed a decrease in ε' above 100°C which were attributed to the loss of bound water or capillary water within the structure of the wood [23]. Al Sayegh et al. also reported similar results, which indicate that dielectric properties are frequency and temperature dependent; they showed a decrease in the dielectric constant of wood beyond 150°C up to 400°C, followed by a slow increase [24].

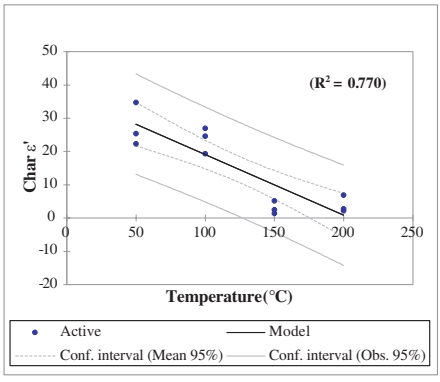

Figure 5. Regression analysis for dielectric constant (ε') values for char.

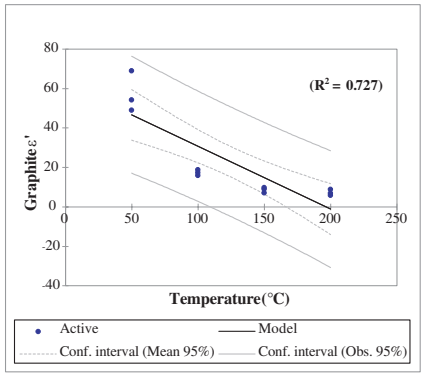

Figure 6. Regression analysis for dielectric constant (ε') values for graphite.

It has been previously shown that microwave heating is enhanced by the presence of a doping agent such as graphitic carbon, a very good microwave absorber. When the free water is lost upon heating, a wood sample without any doping becomes essentially microwave transparent [23, 34, 35]. The findings of the present study further support this theory. The dielectric properties result indicates that char would be a better doping substance than graphite. In order to investigate this further, numerical modeling and a simulation study of the microwave pyrolysis process were carried out by using the char and graphite dielectric properties models.

3.2. Numerical Modeling and Simulation

3.2.1. Meshing

In order to model the effects of doping material on microwave-assisted pyrolysis within the woody biomass, a symmetrical geometry of the entire system as shown in Figure 7 was assumed. The mesh structures of the non-doped and doped systems are presented in Figures 8 and 9. Different mesh element sizes were used for different sub-domains based on the dielectric properties of the sub-domain and the precision required in the sub-domain of interest.

Previous simulation work carried out by the authors has shown that a pyrolysis temperature of 425°C is ideal in obtaining the optimum yield of biochar under microwave-assisted conditions for the given range of temperature [18]. The present objective was to investigate if doping of the wood sample would assist in it reaching desired temperatures in a more efficient manner than non-doped samples. The governing physics for electromagnetic radiation and heat transfer were

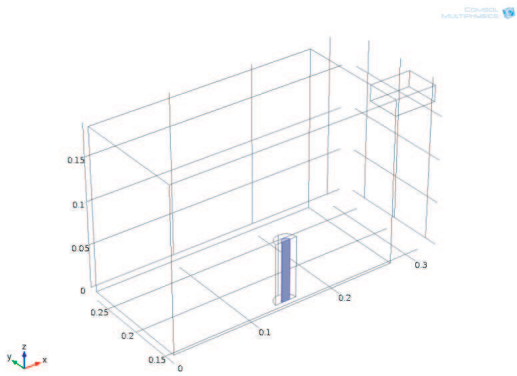

Figure 7. Half sectional view of the reactor configuration with a doped region.

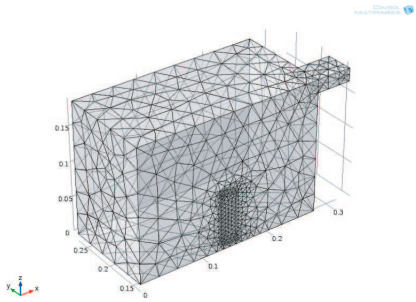

Figure 8. Finite element mesh structure for non-doped biomass (Half sectional view).

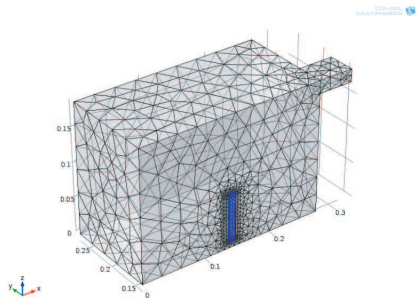

Figure 9. Finite element mesh structure for doped biomass (Half sectional view).

applied for a time range of 15 min (900 s) for each system to determine the temperature distribution within the wood samples.

As seen in Figure 10, the highest temperatures attained for the non-doped wood sample remained below 300°C over the 15 min and showed a heat distribution of $\Delta T^{\circ} \leq 1^{\circ}\text{C}$ within the system. A vertical increase in temperature was observed within the sample with the highest temperature of 296°C occurring at the upper end of the wood and the lowest (295°C) at the bottom.

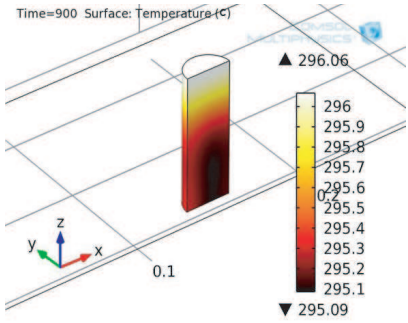

Figure 10. Temperature profile of non-doped biomass for microwave pyrolysis.

The ability of a material to absorb microwave energy is related to its dielectric properties and the average power absorbed by a given volume of material when heated dielectrically is given by Equation (13) [36]:

$$P_{av} = \omega \varepsilon_0 \varepsilon''_{eff} EV \tag{13}$$

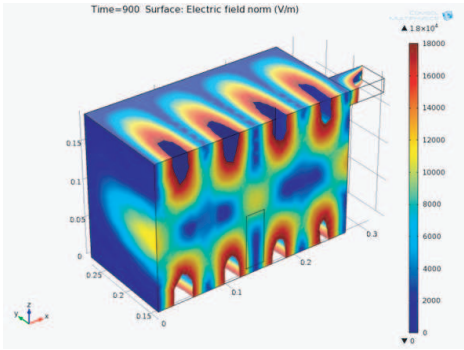

Figure 11. Electric field distribution of non-doped biomass for microwave pyrolysis.

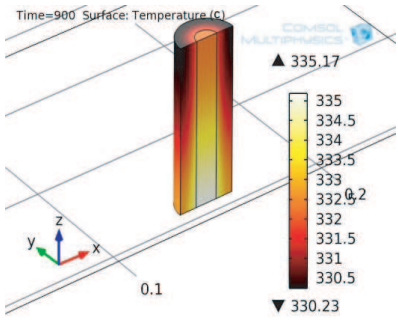

Figure 12. Temperature profile of graphite doped biomass for microwave pyrolysis.

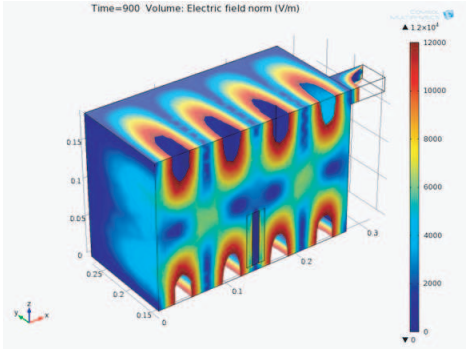

Figure 13. Electric field distribution of graphite-doped biomass for microwave pyrolysis.

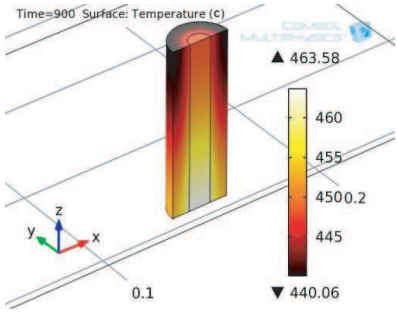

Figure 14. Temperature profile of char doped biomass for microwave pyrolysis.

where P_{av} is the average power absorbed (W); ω is the angular frequency of the generator (rad/s); ε_0 is the permittivity of free space; ε''_{eff} is the effective loss factor; E is the electric field strength (V/m); and V is the volume (m^3). Thus the energy absorbed is proportional to the electric field distribution. The energy within the non-doped biomass sample as governed by the electric field distribution is shown in Figure 11.

In the case of the wood sample doped with graphite, the highest temperature attained after 15 min was $\simeq 335°C$. Heating in this case was less uniform ($\Delta T° \approx 5°C$) across the sample and its vertical progression in the sample was the opposite of that of the non-doped

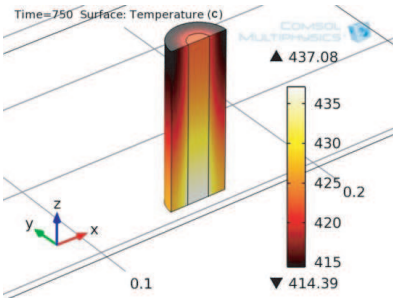

Figure 15. Temperature profile of char-doped biomass for microwave pyrolysis at 13 min.

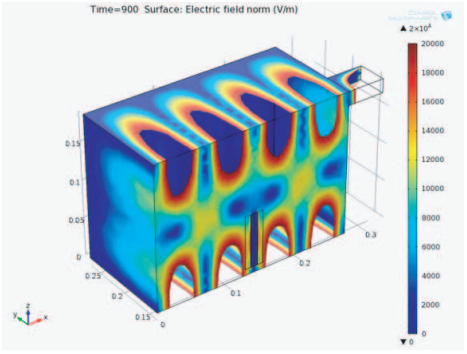

Figure 16. Electric field distribution of char-doped biomass for microwave pyrolysis.

sample (Figure 12). The electric field distribution for the graphite doped sample is shown in Figure 13.

With char-doped biomass, the highest temperature reached after 15 min was 464°C. The vertical heat distribution pattern was similar to that of the graphite-doped biomass, but at overall higher temperatures. The heat distribution ($\Delta T^{\circ} \approx 20^{\circ}$C) was less uniform than for the non-doped and graphite-doped systems (Figure 14). The optimum biochar production temperature of 425°C, determined in a previous simulation study conducted by the same authors [18], was attained by the char-doped biomass within 13 min (Figure 15). The electric field distribution within the system of the char doped sample is shown in Figure 16.

The radiation energy was dissipated within the sample more or less uniformly, giving rise to much greater heating rates, although significant temperature gradients may be established between the hot internal regions and the surface of the sample.

3.3. Experimental Validation

The simulation results indicated that the desired temperature of 425°C was reached within 12.5 min of the onset of the reaction. The change in temperature over this time period was observed to be less than 50°C. This led to the configuration of an experimental design for the experiment. Based on the experimental results, the char-doped samples favored enhanced biochar formation than non-doped or graphite-doped biomass samples. Regression models ($P \leqslant 0.05$) for biochar yields vs. temperature under the three treatments (non-,

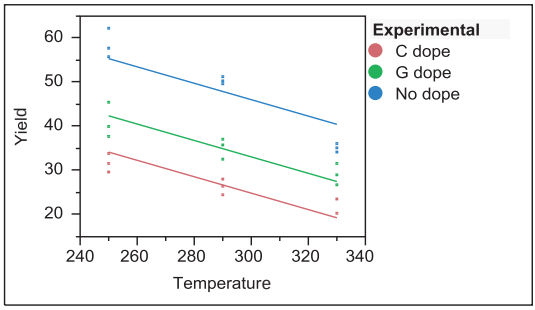

Figure 17. Regression analysis of Yield vs. Temperature ($P \leq 0.01$) for different treatments of biomass sample.

graphite and char-doped) were derived for temperatures of 250°C, 290°C and 330°C (Figure 17). Due to the generation of sparks within the cavity due to microwave interaction with the thermocouple, it was not possible to evaluate the model for temperatures > 330°C.

Figure 14 represents the linear relationship between yield% and temperature for each of the treatments. The correlation of determination for each model indicated that the yield% of the char-doped treatment had the best fit to the model as shown here (Equations (14)–(16)) and illustrated in Figures 18–20. The results also indicated that both the treatment conditions as well as temperature had significant effects on the yields. The effect details through an analysis of variance (ANOVA) are as shown in Table 3.

$$\text{Yield}_{\text{char}} = 60.27 - 0.12T^{\circ} \quad (\mathbf{R^2 = 0.85}) \tag{14}$$

$$\text{Yield}_{\text{graphite}} = 78.25 - 0.15T^{\circ} \quad (\mathbf{R^2 = 0.79}) \tag{15}$$

$$\text{Yield}_{\text{non-doped}} = 134.49 - 0.29T^{\circ} \quad (\mathbf{R^2 = 0.80}) \tag{16}$$

A multiple comparison of yields of the three types of wood samples, treated at three different temperatures (250°C, 290°C and 330°C) was conducted through an ANOVA and Duncan's Multiple Range test ($P \leq 0.05$). The ANOVA results are presented in Table 4. Char-doping at 330°C showed the lowest biochar yield than either of the other two doping treatments at that temperature (Figure 21) while treatments of 250°C produced greatest yields. However, biochar yields of non-doped biomass treated at 330°C and graphite-doped biomass treated at 290°C were not significantly different ($P > 0.05$).

The results of the present study prove the effect of pyrolysis temperatures on the final biochar yield. It can be seen from Figure 18 that with increase in temperature, biochar yields decrease. Similar observations have been reported by several research studies [37–40].

Table 3. Effect tests results for multiple comparison of yields of the three types of wood samples.

Source	Nparm	DF	Sum of squares	F	Pr >F
Temperature	1	1	622.2291	47.2854	< 0.0001
Experimental condition	2	2	1525.2809	57.9558	< 0.0001

Table 4. Analysis of variance (ANOVA) results for multiple comparison of yields of the three types of wood samples .

Source	DF	Sum of squares	Mean squares	F	Pr >F
Model	8	3221.882	402.735	55.595	<0.0001
Error	18	130.393	7.244		
Corrected Total	26	3352.275			

Microwave pyrolysis of corn cob carried out at temperatures ranging from 300 to 600°C indicated that the char yield decreased significantly to 23% with an increase in temperature to 600°C [37]. The effect of treatment conditions such as temperature, particle size, and lignin and inorganic matter contents on bio-char yield and reactivity were investigated by Demirbas (2004) [38]. The results of the elemental analysis show that high temperature and smaller particles led to an increase in the heating rate resulting in a decreased bio-char yield. On the other hand, carbon contents in the biochar increase with pyrolysis temperature.

The present experimental results clearly corroborate the simulations, and confirm the hypothesis that as a microwave receptor doping of biomass could have an influence on the pyrolysis products. Doping of the wood was instrumental in sustaining greater temperature uniformity and faster heating rates, thus improving the material's pyrolysis rate. Previous studies have indicated that the incorporation of receptors in the material can also be used to modify the pyrolysis process for maximization of a particular pyrolysis product [35]. The

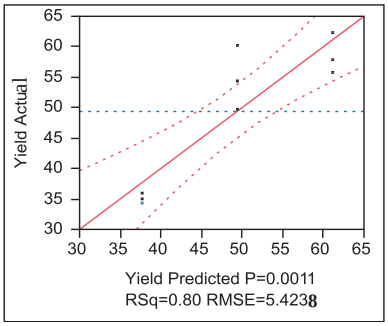

Figure 18. Regression analysis of Actual vs. Predicted biochar yields ($P \leq 0.01$) for non doped biomass sample.

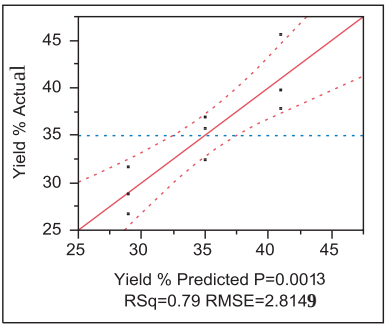

Figure 19. Regression analysis of Actual vs. Predicted biochar yields ($P \leq 0.01$) for graphite doped biomass sample.

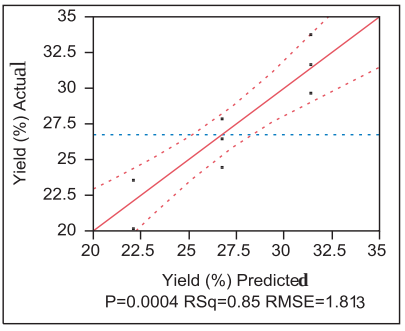

Figure 20. Regression analysis of Actual vs. Predicted biochar yields ($P \leq 0.01$) for char doped biomass sample.

effects of char and graphite as microwave receptors on yield and the properties of oil products was investigated by Domínguez et al. [41]. Their results indicated that the bio-oil yields obtained from microwave pyrolysis with char as a receptor were higher than those obtained with graphite. Moreover, they showed that the use of graphite instead of char as a microwave receptor favored the cracking of large aliphatic chains to lighter species of oil products. Previous studies have shown that the solid residue or char produced through the pyrolysis also contributes to the final pyrolysis temperature. Therefore, the use of char as a doping agent could prove to be useful [35].

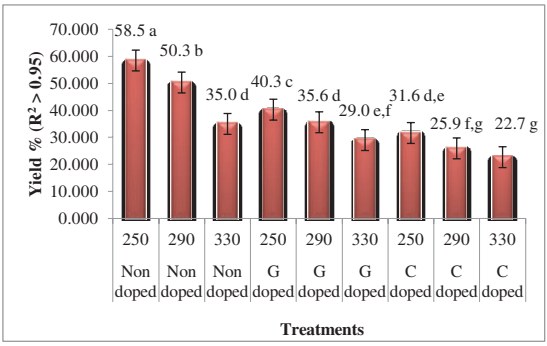

Figure 21. Duncan's multiple range test comparative analysis of experimental microwave pyrolysis yields representing statistical significance among the treatments. The means followed by the same letter are not significant at $P \leq 0.05$ level .

4. CONCLUSIONS

This study investigated the advantages of using doping agents such as char and graphite to improve heat transfer during microwave pyrolysis of lignocellulosic biomass. A finite element model (FEM) was developed using the dielectric properties of the doping agents. The regression models developed from the dielectric property measurements indicated that char doping was better suited for microwave heating than graphite. The model developed during the simulation study found that doping helped to achieve a more efficient heat transfer within the biomass compared to non-doped samples. Char-doping resulted in rapidly reaching optimal temperatures, resulting in greater biochar yields. Laboratory-scale trials were conducted to test the validity and effectiveness of the simulation results. Statistical analysis of the yields of the biochar indicated that char doping was very efficient in terms of reducing heating time and raising temperature compared to graphite doping. The numerical simulation model could be used to inform the design of a microwave-assisted bioreactor capable of achieving maximum biochar formation.

ACKNOWLEDGMENT

The authors would like to gratefully acknowledge the financial support of NSERC (Natural Sciences and Engineering Research Council), Canada, Le Fonds de recherche du Québec — Nature et technologies (FQRNT) and Schulich Canada Graduate Scholarships.

REFERENCES

1. Intergovernmental Panel on Climate Change (IPCC), "IPCC fourth assessment report: Climate change 2007," 2007, accessed on June 28, 2013, http://www.ipcc.ch/publications_and_data/publications_and_data_reports.shtml#1.
2. Climate Change, Government of Canada, "Canada's action on climate change," 2013, accessed on June 28, 2013, http://www.climatechange.gc.ca/default.asp?lang=En&n=72F16A84-1.
3. Environment Canada, "National inventory report 1990–2011: Greenhouse gas sources and sinks in Canada — Executive summary," 2013, accessed on June 28, 2013, http://www.ec.gc.ca/ges-ghg/default.asp?lang=En&n=68EE206C-1&offset=1&toc=show.
4. Agriculture and Agri Food Canada (AAFC), "Agriculture residue," 2008, accessed on June 28, 2013, http://www4.agr.gc.ca/AAFC-AAC/display-afficher.do?id=1226510406028&lang=eng.
5. Statistics Canada, "Human activity and the environment: Annual statistics," Catalogue No. 16-201-X, 2009, accessed on June 28, 2013, http://www.statcan.gc.ca/pub/16-201-x/16-201-x2009000-eng.pdf.
6. Wu, H. and H. Abdullah, "Biochar as a fuel: 1. Properties and grindability of biochars produced from the pyrolysis of Mallee wood under slow-heating conditions," *Energy & Fuels*, Vol. 23, No. 8, 4174–4181, 2009, DOI: 10.1021/ef900494t.
7. Lehmann, J., "Bio-energy in the black," *Frontiers in Ecology and the Environment*, Vol. 5, No. 7, 381–387, 2007, DOI: 10.1890060133.
8. Joseph, S., C. Peacocke, J. Lehmann, and P. Munroe, "Developing a biochar classification and test methods," *Biochar for Environmental Management, Science and Technology*, J. Lehmann (ed.), 107–126, Earthscan, London, VA, 2009.
9. Kleiner, K., "The bright prospect of biochar," *Nature Reports Climate Change*, No. 3, 2009, DOI:10.1038/climate.2009.48.
10. International Biochar Initiative (IBI), "Biochar is a valuable soil additive," 2010, accessed on June 28, 2013, http://www.biochar-international.org/biochar.
11. Brownsort, P. A., "Biomass pyrolysis processes: Performance parameters and their influence on biochar system benefits," M.Sc. thesis, School of Geosciences, University of Ed-

inburgh, Edinburgh, UK, 2009, accessed on June 28, 2013, http://hdl.handle.net/1842/3116.

12. Dutta, B., G. S. V. Raghavan, and M. Ngadi, "Surface characterization and classification of slow and fast pyrolysed biochar using novel methods of pycnometry and hyper-spectral imaging," *Journal of Wood Chemistry and Technology*, Vol. 32, No. 2, 105–120, 2011, DOI: 10.1080/02773813.2011.607535.
13. Copson, D. A., *Microwave Heating*, 2nd Edition, xi-615, Avi Pub. Co., Westport, Conn., 1975.
14. Metaxas, A. C., *Foundations of Electroheat. A Unified Approach*, 400, John Wiley & Sons, Baffins Lane, Chichester, West Sussex, 1996.
15. Thostenson, E. T. and T. W. Chow, "Microwave processing: Fundamentals and applications," *Composites: Part A*, Vol. 30, 1055–1071, 1999.
16. Babu, B. V. and A. S. Chaurasia, "Pyrolysis of biomass: Improved models for simultaneous kinetics and transport of heat, mass and momentum," *Energy Conversion and Management*, Vol. 45, No. 9–10, 1297–1327, 2004, DOI: 10.1016/j.enconman.2003.09.013.
17. Blasi, D., "Comparison of semi-global mechanisms for primary pyrolysis of lignocellulosic fuels," *Journal of Analytical and Applied Pyrolysis*, Vol. 47, No. 1, 43–64, 2008, DOI: 10.1016/S0165-2370(98)00079-5.
18. Dutta, B., S. R. S. Dev, Y. Gariépy, and G. S. V. Raghavan, "Finite element modelling of microwave pyrolysis of biomass," *Proceedings of 7th International Conference on Heat Transfer, Fluid Mechanics and Thermodynamics (HEFAT)*, Antalya, Turkey, July 19–21, 2010.
19. Dev, S. R. S., Y. Gariépy, and G. S. V. Raghavan, "Measurement of dielectric properties and finite element simulation of microwave pretreatment for convective drying of grapes," *PIERS Online*, Vol. 5, No. 7, 690–695, 2009.
20. Delisle, G. Y., K. L. Wu, and J. Litva, "Couples finite element and boundary element method in electromagnetics," *Comp. Phys. Commun.*, Vol. 68, No. 1–3, 255–278, 1991, DOI: 10.1016/0010-4655(91)90203-W.
21. Dev, S. R. S., Y. Gariépy, V. Orsat, and G. S. V. Raghavan, "FDTD modeling and simulation of microwave heating of in-shell eggs," *Progress In Electromagnetics Research M*, Vol. 13, 229–243, 2010.

22. Sanga, E. C. M., "Microwave assisted drying of composite materials: Modelling and experimental validation," Dissertation — Master's Thesis, McGill University, 2002.
23. Robinson, J. P., S. W. Kingman, R. C. Barranco, E. Snape, and H. Al-Sayegh, "Microwave pyrolysis of wood pellets," *Ind. Eng. Chem. Res.*, Vol. 49, No. 2, 459–463, 2010, DOI: 10.1021/ie901336k.
24. Al-Sayegh, H., J. Robinson, G. Dimitrakis, and S. Kingman, "Microwave processing of forestry waste," *IET RF and Microwave Network and National Centre for Industrial Microwave Processing (NCIMP)*, University of Nottingham, UK, December 2, 2010.
25. Domínguez, A., M. A. Menéndez, et al., "Conventional and microwave induced pyrolysis of coffee hulls for the production of a hydrogen rich fuel gas," *J. Anal. Appl. Pyrolysis*, Vol. 79, No. 1–2, 128–135, 2007, DOI: 10.1016/j.jaap.2006.08.003.
26. Goss, W. P. and R. G. Miller, "Thermal properties of wood and wood products," *Proceedings of the Thermal Performance of the Exterior Envelopes of Whole Buildings International Conference*, Oak Ridge national Laboratory, Department of Energy, USA, 1992, accessed on September 25, 2013, http://web.ornl.gov/sci/buildings/2012/1992%20B5/028.pdf.
27. Center for Solid State Science, "Mass density in Engineered materials," Arizona State University, accessed on September 25, 2013, http://invsee.asu.edu/nmodules/engmod/propdensity.html.
28. Picard, S., D. T. Burns, and P. Roger, "Measurement of the specific heat capacity of graphite," *Rapport BIPM-2006/01*, International Bureau of Weights and Measures, France, 2006. Available at: www.bipm.org/utils/common/pdf/rapportBIPM/2006/01.pdf, accessed on October 11, 2013.
29. Clark, R. N., "Dielectric properties of materials," *Kaye and Laby Online: Tables of Physical and Chemical Constants,* National Physical Laboratory, Middlesex, UK, 1995, accessed on September 25, 2013, http://www.kayelaby.npl.co.uk/general_physics/2_6/2_6_5.html.
30. Ida, N., "Magnetic properties of materials," *Engineering Electromagnetics*, Springer, USA, 2004.
31. Ayappa, K. G., H. T. Davis, E. A. Davis, and J. Gordon, "Two-dimensional finite element analysis of microwave heating," *AIChE Journal*, Vol. 38, No. 10, 1577–1592, 1992, DOI: 10.1002/aic.690381009.
32. Zheng, F., Z. Chen, and J. Zhang, "Toward the development of a three-dimensional unconditionally stable finite-difference

time-domain method," *IEEE Transactions on Microwave Theory And Techniques*, Vol. 48, No. 9, 1550–1558, 2000, DOI: 10.1109/22.869007.

33. COMSOL Multiphysics, "Chemical reaction engineering module (Version 4.1a)," Burlington, MA, USA, 2012, available at: http://www.comsol.com/.
34. Zuo, W., Y. Tian, and R. Ren, "The important role of microwave receptors in bio-fuel production by microwave-induced pyrolysis of sewage sludge," *Waste Management*, Vol. 31, 1321–1326, 2011.
35. Fernández, Y., A. Arenillas, and J. Á. Menéndez, "Microwave heating applied to pyrolysis," *Advances in Induction and Microwave Heating of Mineral and Organic Materials*, 724–752, Stanisław Grundas, Ed., Intech., Rijeka, Croatia, 2011, DOI: 10.5772/13548.
36. Oloyede, A. and P. Groombridge, "The influence of microwave heating on the mechanical properties of wood," *Journal of Materials Processing Technology*, Vol. 100, 67–73, 2000.
37. Yu, F., P. H. Steele, and R. Ruan, "Microwave pyrolysis of corn cob and characteristics of the pyrolytic chars," *Energy Sources*, Part A, Vol. 32, 475–484, 2010.
38. Demirbas, A., "Effects of temperature and particle size on bio-char yield from pyrolysis of agricultural residues," *J. Anal. Appl. Pyrolysis*, Vol. 72, 243–248, 2004.
39. Dutta, B., "Assessment of pyrolysis techniques of lignocellulosic biomass for biochar production," Dissertation — Master's Thesis, McGill University, 2010.
40. Uemura, Y., W. N. Omar, S. Razlan, H. Mif, S. Yusup, and K. Onoe, "Mass and energy yields of bio-oil obtained by microwave-induced pyrolysis of oil palm kernel shell," *Journal of the Japan Insdture of Energy*, Vol. 91, 954–959, 2012.
41. Domínguez, A., J. A. Menéndez, M. Inguanzo, P. L. Bernad, and J. J. Pis, "Gas chromatographic-mass spectrometric study of the oil fractions produced by microwave-assisted pyrolysis of different sewage sludges," *Journal of Chromatography A*, Vol. 1012, No. 2, 193–206, 2003, DOI: 10.1016/S0021-9673(03)01176-2.